Eur Biophys J (2006) 35: 293–301
DOI 10.1007/s00249-005-0034-6

ARTICLE

Anthony D. Maher · Bogdan E. Chapman · Philip W. Kuchel

^{39}K nuclear magnetic resonance and a mathematical model of K^+ transport in human erythrocytes

Received: 25 July 2005 / Revised: 31 October 2005 / Accepted: 13 November 2005 / Published online: 10 December 2005
© EBSA 2005

Abstract ^{39}K nuclear magnetic resonance was used to measure the efflux of K^+ from suspensions of human erythrocytes [red blood cells (RBCs)], that occurred in response to the calcium ionophore, A23187 and calcium ions; the latter activate the Gárdos channel. Signals from the intra- and extracellular populations of $^{39}K^+$ were selected on the basis of their longitudinal relaxation times, T_1, by using an inversion- recovery pulse sequence with the mixing time, τ_1, chosen to null one or other of the signals. Changes in RBC volume consequent upon efflux of the ions also changed the T_1 values so a new theory was implemented to obviate a potential artefact in the data analysis. The velocity of the K^+ efflux mediated by the Gárdos channel was 1.19 ± 0.40 mmol (L RBC)$^{-1}$ min^{-1} at 37°C.

Keywords ^{39}K nuclear magnetic resonance · K^+ transport · Erythrocyte · Membrane transport · *Mathematica*

Abbreviations AAS: Atomic absorption spectroscopy · DE: Differential equation · DMSO: Dimethyl sulfoxide · DyPPP: Dysprosium tripolyphosphate · HBS: HEPES-buffered saline · Hb: Haemoglobin · Ht: Haematocrit · MCHC: Mean corpuscular haemoglobin concentration · MRI: Magnetic resonance imaging · NMR: Nuclear magnetic resonance · ODE: Ordinary differential equation · RBC: Red blood cell · RO: Reverse osmosis · SSA: Sickle cell anaemia · T_1: Longitudinal relaxation time · TCA: Trichloroacetic acid

A. D. Maher · B. E. Chapman · P. W. Kuchel (✉)
School of Molecular and Microbial Biosciences,
University of Sydney, 2006 Sydney, NSW, Australia
E-mail: p.kuchel@mmb.usyd.edu.au
Tel.: +61-2-93513709
Fax: +61-2-93514726

Introduction

Transmembrane K^+ fluxes in suspensions of human erythrocytes [red blood cells (RBCs)] can be measured non-invasively and non-destructively using nuclear magnetic resonance (NMR) spectroscopy. This was originally made possible by the introduction of dysprosium-based paramagnetic shift reagents, including $[Dy(PPP)_2]^{7-}$ (Gupta and Gupta 1982; Pike et al. 1982, 1985) that facilitate the resolution of intra- and extracellular cation spectral peaks. While there appear to be minimal adverse effects of the shift reagents on cell morphology and physiology (Knubovets et al. 1989; Pettegrew et al. 1984) there are some, at least potential, objections to using shift reagents in studies of membrane transport. Nevertheless, these compounds have been widely used to differentiate transmembrane cation populations in many tissues (e.g., Shedd and Spicer 1991). More recently, such reagents have been introduced into magnetic resonance imaging (MRI) as relaxation-contrast agents (Preston and Foster 1993; Weidensteiner et al. 2002). It was significant for studies of membrane transport that the requirement for shift reagents could be circumvented (Seo et al. 1987). The latter authors demonstrated selective detection of intracellular $^{39}K^+$ in perfused rat salivary glands by using a modified inversion-recovery pulse sequence; this exploits the difference in T_1 relaxation times between the $^{39}K^+$ nuclei in the two compartments. The method was applied to measure acetylcholine-stimulated $^{39}K^+$ fluxes in salivary cells and rat hearts (Kuki et al. 1990; Murakami et al. 1989). Inversion-recovery pulse sequences are used routinely in MRI to weight selectively nuclei in specific compartments (Bydder 1992; Bydder et al. 1998; Kates et al. 1996; Newhouse 1986). Another method of detecting a cation signal from only the inside or outside of cells is the selective detection of a resonance corresponding to double-quantum coherence from relatively immobile ions. This has been done for the intracellular $^{39}K^+$ in rat salivary glands, and cardiomyocytes (Hiraishi et al.

1990; Seo et al. 1990). However, the length of time taken to record each spectrum (~13.7 h) prohibits the capture of kinetic events that occur on the minute timescale.

Human RBCs have K^+ channels, Gárdos channels, that are activated by Ca^{2+}. Under normal physiological conditions, the Ca^{2+} concentration inside the cells is below the threshold value that activates the channel [2–3 μM; (Yingst and Hoffman 1984)]. However, in the event of Ca^{2+} elevation, the plasma membrane becomes very permeable to K^+. It is this outcome that is responsible for the K^+ loss and hence dehydration of RBCs in patients with sickle cell anaemia (SSA) (Brugnara 1995; Brugnara et al. 1986).

Here, we report the application and development of the inversion-recovery pulse sequence as a method for measuring the kinetics of net K^+ fluxes in suspensions of human RBCs in the context of Gárdos channel activation. The presented method is different from those previously reported in that it accounts for complications introduced by changes in cell volume during the measurement, and allows for measurement of $^{39}K^+$ outside the cells. Furthermore, the approach has been analysed by a mathematical model of the system that accounts for differences in the rate constant estimates made by using an established technique, atomic absorption spectroscopy (AAS), and the NMR method.

Materials and methods

Materials

All fine chemicals were used as received from Sigma (St. Louis, MO, USA)

Buffers and solutions

HEPES-buffered saline (HBS: 145 mM NaCl, 20 mM HEPES, 5 mM KCl and 0.1 mM penicillin, pH 7.4) was filtered three times through a 0.45-μm nitrocellulose membrane (Micro Filtration Systems, CA, USA) to remove insoluble contaminants. The osmolality was adjusted, using NaCl, to 290 ± 3 mmol kg^{-1} with a Vapro® Vapor Pressure Osmometer 5520 (Wescor, UT, USA)

Concentrated stock solutions of A23187 were prepared in dimethyl sulfoxide (DMSO). All other solutions were prepared in reverse osmosis (RO) water.

Red blood cell preparation

Blood (~20 mL) was withdrawn by venipuncture from the cubital fossa of healthy donors into heparin [15 U (mL whole blood)$^{-1}$] and immediately centrifuged at 4°C for 5 min at 3,000 *g* in a swing-out rotor (Jouan centrifuge, CR4-12, France). The plasma and the buffy coat were aspirated. The cells were resuspended in ~4 vol. of HBS, re-centrifuged and resuspended in ~3 vol. of HBS. CO was gently bubbled through the suspension for 5 min to render the haemoglobin (Hb) into a stable diamagnetic state favourable for NMR studies. Cells were then centrifuged and resuspended in ~1 vol. of HBS supplemented with 10 mM glucose, 0.1 mM ouabain (to inhibit the Na^+, K^+—ATPase) and 0.05 mM bumetanide and 0.05 mM furosemide (to inhibit the $Na^+/K^+/2Cl^-$ and K^+/Cl^- cotransporters) and used within 24 h. All experiments were performed at 37°C.

Atomic absorption spectroscopy

Time-courses of the cation transport were initiated by adding the desired ionophore to the RBC suspension containing the cation. At pre-determined times, 100-μL duplicate samples of RBC suspension were layered over 200 μL of dibutyl phthalate oil in a 1.5-mL Eppendorf plastic centrifuge tube. Because the density of dibutylphthalate (~1.042–1.045 at 20°C) is less than that of the cells, but greater than that of the supernatant, RBCs are separated from the extracellular fluid by rapid centrifugation (12,000 *g*, model 5412 Eppendorf, Gerätebau, West Germany) in less than 5 s (Joyner and Kirk 1994); this effectively stops the reaction at the time of spinning. The result is three distinct layers: the top layer being the extracellular fluid, the middle layer, dibutyl phthlate, and the bottom, the cells.

For the measurement of $[K^+]_{out}$ by AAS a 200-μL aliquot of the top layer was diluted in 5 mL of RO water. For the measurement of $[K^+]_{in}$, the remaining supernatant and dibutyl phthlate were aspirated and the cell pellet resuspended in 1 mL of RO water (to lyse the cells) and then 0.3 mL of 10% (w/v) Trichloroacetic acid (TCA) was added to precipitate the Hb. This sample was vortexed and centrifuged at 12,000 *g* for 15 min. A 200-μL portion of the resulting supernatant was diluted by a factor of 50 in RO water, resulting in an ion concentration within the measurable range of 0.02–2.00 μg mL^{-1}.

A Varian SpectrAA-10/20 atomic absorption spectrometer, with a Na/K hollow cathode dual lamp (Varian, Mulgrave, Vic, Australia), was used for all measurements.

Nuclear magnetic resonance spectroscopy

All NMR experiments were performed on a Bruker (Karlsruhe, Germany) DRX 400 vertical wide-bore spectrometer using 10-mm sample tubes (Wilmad, Buena, NJ, USA) made of glass. ^{39}K spectra were acquired at 18.67 MHz. Typically, 3-mL samples were used and after tuning and matching the probe a 1D spectrum was acquired using an inversion-recovery pulse sequence, D_1-180°-τ_1-90°—acquire, where D_1 denotes a delay of 5 T_1 values, and τ_1 denotes the longitudinal-magnetization

relaxation delay. Time-courses were initiated by direct addition of A23187 and $CaCl_2$ (to a final concentration of 22 μM and 2 mM outside the cells, respectively) to the tube after its ejection from the spectrometer. A23187 mediates the elecroneutral exchange of Ca^{2+} for $2H^+$. The sample was mixed by threefold end-to-end inversion and placed back into the spectrometer. Data acquisition began within 1 min. A co-axial capillary containing D_2O was used for field/frequency locking. For each time point, 64 or 128 transients were collected into 8,192 data points. Prior to Fourier transformation, the free-induction decay was multiplied by an exponential line-broadening factor of 5 Hz. The spectra were phased, baseline-corrected and referenced to the ^{39}K resonance (ppm = 0.00).

Further spectral processing, including peak integration, was carried out using XWINNMR (Bruker).

Haematocrit determination

RBC suspensions were drawn into commercially supplied 1×75 mm heparin-coated glass capillary tubes using a 1-mL syringe and an adaptor tube. The capillary was sealed with putty and centrifuged for 8 min in a capillary centrifuge (Clements Micro Haematocrit, Sydney, NSW, Australia). The Ht was then determined with the aid of a Micro Haematocrit Reader (Hawksley, England). In other experiments, the haematocrit was measured automatically using a Sysmex KX-21 cell counter (Sysmex, Kobe, Japan).

Mathematical models

Mathematical models describing the time-dependence of the amounts and concentrations of relevant ions and solutes inside and outside the cells were programmed in *Mathematica* (Wolfram Research, Champaign, IL, USA), using the methods described in Mulquiney and Kuchel (2003).

A schematic representation of the key biophysical and biochemical reactions considered by the model is given in Fig. 1.

The first step in the construction of the model in *Mathematica* was to define the initial conditions of the system such as Ht, suspension volume, concentrations of principle ions, etc., followed by the equations for the initial volumes of the water-accessible compartments (it was considered essentially a two compartment system) in terms of these. It was assumed that only 70% of the intracellular volume was accessible to water (the remainder being occupied by haemoglobin).

The model took into account that significant volume changes occur as a result of the net ion flux between the two compartments (osmotically susceptible water being rapidly transported via transmembrane aquaporins). Equations that incorporate volume as a dependent variable into the model were derived from the osmotic pressure condition, which states that the sum of the concentrations of the solutes on either side of the membrane are equal:

$$\text{sum of concentrations inside} = \text{sum of concentrations outside.} \quad (1)$$

It follows that

$$\frac{\text{sum of mol of solute inside}}{\text{Vol}_{\text{in}}} = \frac{\text{sum of mol of solute outside}}{\text{Vol}_{\text{out}}}, \quad (2)$$

where mol stands for moles and Vol stands for volume, and

$$\text{Vol}_{\text{in}} = \frac{(\text{sum of mol of solute inside})\,(\text{Vol}_{\text{out}})}{\text{sum of mol of solute outside}}, \quad (3)$$

but $\text{Vol}_{\text{total}} = \text{Vol}_{\text{in}} + \text{Vol}_{\text{out}}$, so,

$$\text{Vol}_{\text{in}} = \frac{(\text{sum of mol of solute inside})\,(\text{Vol}_{\text{total}} - \text{Vol}_{\text{in}})}{\text{sum of mol of solute outside}}, \quad (4)$$

which upon rearrangement becomes

$$\text{Vol}_{\text{in}} = \frac{(\text{sum of mol of solute inside})\,(\text{Vol}_{\text{total}})}{\text{sum of mol of solute out} + \text{sum of mol of solute inside}}. \quad (5)$$

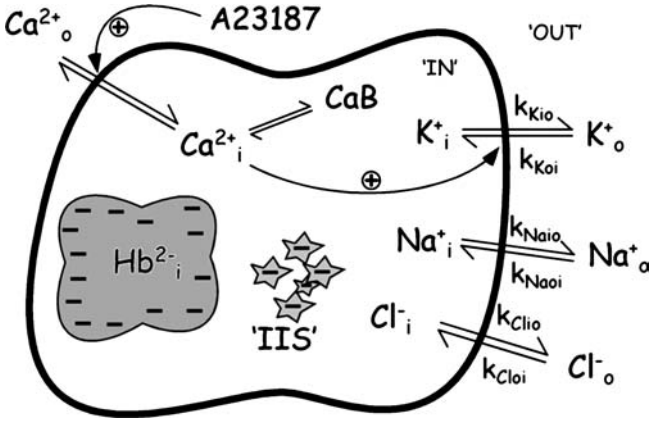

Fig. 1 Scheme describing the activation of the Gárdos channel in a suspension of RBCs. A23187 equilibrates Ca^{2+} across the membrane. The model (see Appendix) includes equations to describe the transmembrane fluxes of K^+, Na^+ and Cl^-, noting that K^+ flux is sensitive to $[Ca^{2+}]_{in}$. Thirty percent of the intracellular volume is occupied by Hb (which has a net charge of -2 at pH 7.2), along with other impermeant intracellular solutes (*IIS*). The model distinguishes between intra- and extracellular ions (compartments '*IN*' and '*OUT*', respectively, denoted also by *subscripts* '*i*' and '*o*'). *Unitary rate constants* are represented as '$k_{\text{subscript}}$' where 'subscript' = the ion + direction of flux (where *io* = 'in to out direction' and vice versa). *CaB* denotes bound (inactive) Ca^{2+}

It follows that the equation for the volume outside (in a two-compartment system) is simply the difference between the total volume and the volume inside.

Unitary rate constants for K^+ flux through the channel were defined in accordance with the experimentally determined values, as was a constant for half-maximal activation of the channel by Ca^{2+}_{in}. The rate of Na^+ transport through the channel was defined to be 0, while the net transport of Cl^- across the membrane was considered sufficiently rapid to maintain electroneutrality. These rate constants were corrected for Cl^- distribution effects (Rohwer et al. 2002).

A set of differential equations (DEs) was defined for each reaction (chemical and physical) and numerically solved using the built-in NDSolve function. Time-courses showing the predicted changes in concentrations, etc., for each species were then generated. A more detailed description of the construction of the model is given in the Appendix, and the *Mathematica* notebook is available from the authors.

Results

Selective observation of intracellular K^+

In order to observe selectively intracellular K^+ using an inversion-recovery pulse sequence, it is first necessary to determine the 'null point' for the signal from the extracellular nuclei. A series of ^{39}K NMR spectra were obtained from a HBS solution using the inversion-recovery pulse sequence, with τ_1 ranging over 16 values between 10 and 200 ms. Following phasing and baseline correction, a set of intensities at each increment of τ_1 could be generated from the series of spectra by peak integration. The T_1 value was calculated by nonlinear regression of the equation $S(t) = S(\infty) - (S(\infty) - S(0))\, e^{-t_1/T_1}$ onto the data [where $S(\infty)$ is the equilibrium signal, and τ is the 'z-axis time' of the magnetization vector] using either XWINNMR or *Mathematica*. The 'null point' (where $S(t) = 0$, i.e., $T_1 \times \log_e 2$) was found to be 40 ms by this method (data not shown).

When this inversion-recovery pulse sequence was applied to a suspension of RBCs, a single resonance was observed from the intracellular K^+. Fig. 2a shows the change in the ^{39}K NMR signal from a suspension of RBCs following the addition of A23187 and Ca^{2+}. A gradual decrease in the intensity of the resonance was observed. The amount of intracellular K^+ was calculated from the peak integral by assuming conservation of mass and using an initial estimate of $[K^+]_{in}$ of 140 mM. This concentration corresponded to an initial intracellular amount of K^+ of 160 µmol in the whole sample. Figure 2b shows the amount of K^+ inside the cells in the sample. The data were grouped so as to minimize the effects of noise in the spectra. An initial rate of efflux from the cells of 0.74 ± 0.29 µmol min^{-1} was calculated by fitting a degree-2 polynomial to the data.

Selective observation of extracellular K^+

In order to observe selectively the extracellular K^+, the T_1, for the intracellular $^{39}K^+$ was measured in a suspension of RBCs in a K^+-free medium. A 'null point' of $\tau_1 = 11.7$ ms was calculated from the 16 separate spectra shown in Fig. 3, from which T_1 was estimated by regression analysis to be 16.9 ms.

Figure 4a shows a series of ^{39}K NMR spectra from the RBCs in K^+-free medium, acquired with $\tau_1 = 11.7$ ms. The Ca^{2+}-specific ionophore A23187 was added to the suspension at $t = 0$. There was an immediate and pronounced systematic increase in the intensity of the extracellular ^{39}K NMR resonance over the next 80 min, corresponding to the efflux of the ions. (Note that these spectra were phased to give upright peaks because in the inversion-recovery experiment, the magnetization of the more slowly relaxing extracellular $^{39}K^+$ has its vector still in the -z direction before the 90° pulse and hence in the -y direction after it.)

Figure 4b shows a graph of the time-course of the amount of extracellular $^{39}K^+$ as measured by integra-

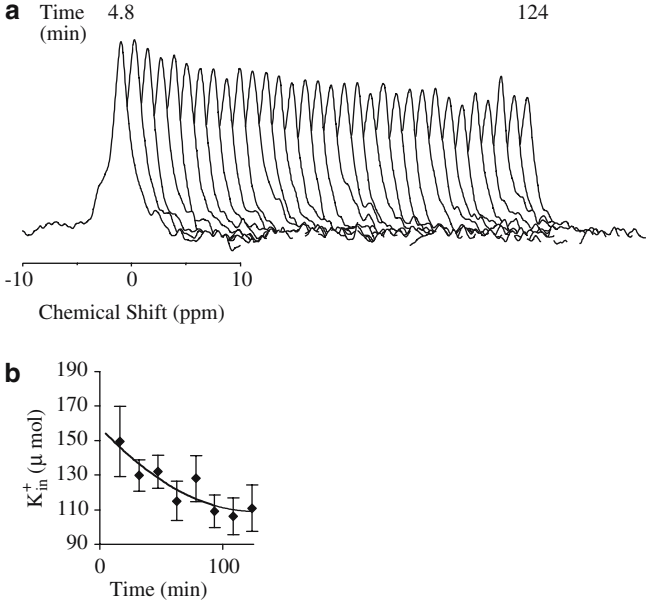

Fig. 2 Time-dependence of signal-averaged $^{39}K^+$ NMR signal from a suspension of human RBCs acquired using an inversion-recovery pulse sequence. A volume of 3 mL of washed RBCs (Ht = 0.54) were placed in a 10-mm NMR tube in glucose-free HBS in the spectrometer and a ^{39}K spectrum recorded every 3.5 min. These spectra were acquired with the pulse sequence D_1–180°-τ_1–90° acquire, where $D_1 = 300$ ms and $\tau_1 = 40$ ms. After ~1 h, 30 µL of 0.8 mM A23187 in DMSO and 30 µL of 100 mM $CaCl_2$ were added to the suspension, the cells placed back in the spectrometer, and ^{39}K spectra were recorded for a further ~1.5 h. **a** time-course of the ^{39}K NMR spectra after addition of A23187 and $CaCl_2$. **b** apparent amount of K^+ inside the cells calculated from the integral of the ^{39}K resonance, assuming that the initial $[K^+]_{in} = 140$ mM. By fitting quadratic functions to the data, an estimate of the initial rate of efflux for K^+ of 0.74 ± 0.29 µmol min^{-1} was determined. Data values were the average from four consecutive spectra. *Error bars* represent ± 1SD

tion of this resonance (*filled squares*). A similar experiment in which K^+ was measured by AAS is also shown (*filled diamonds*). There was a large discrepancy between the calculated time-course for K^+_{out} estimated by the two methods (0.213 ± 0.084 mmol (L RBCs)$^{-1}$ min^{-1} for NMR, compared to 1.19 ± 0.40 mmol (L RBCs)$^{-1}$ min^{-1} for AAS).

Measurement of both pools of K^+ and juxtaposition with AAS data

Semi-simultaneous recordings of changes in intra- and extracellular $^{39}K^+$ were made possible by interleaving the spectra obtained with τ_1 values alternating between 40 and 11 ms. Thus, there was an alternate recoding of the intra- and extracellular $^{39}K^+$ signals. Hence, Fig. 5 shows the amounts of $^{39}K^+$ beginning with an initial content of 160 μmol inside and 6 μmol outside the RBCs, in the whole sample.

When AAS was used to measure K^+ outside the cells, the results were again significantly different from those obtained with NMR. Figure 5 reflects the extent to which the NMR method underestimated the amount of K^+_{out}, while overestimating the amount of K^+_{in}. This artefact was surmised to be due to the cells becoming dehydrated as K^+ effluxed from them (see next section). The increase in [Hb] would have led to a decrease of T_1 inside the cells. Hence, the more rapid relaxation of the intracellular nuclei would then have led to a failure of the intracellular signal to be nulled at the prescribed value of τ_1, when the 90° pulse was applied. By the same argument, the amounts of intracellular K^+ calculated by this method were progressively overestimated as [Hb] increased inside the cell due to loss of cell water. Thus, to enhance the value of this NMR approach, the dependence of T_1 on [Hb] was measured as described next, and the results were incorporated into a mathematical model that accounted for the discrepancies between the data.

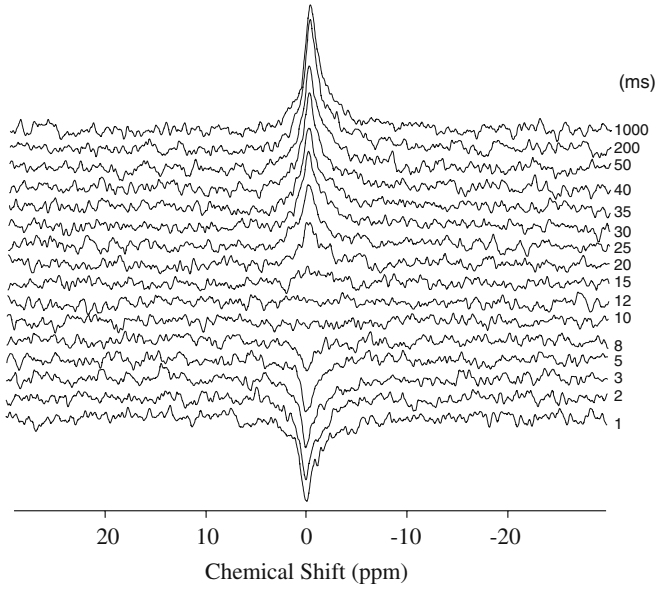

Fig. 3 Series of ^{39}K NMR inversion-recovery spectra obtained from a suspension of human RBCs with the indicated τ_1 values (ms); 3 mL of washed RBCs were suspended in HBS supplemented with 10 mM glucose (Ht = 0.65). The delay before the pulse sequence was 300 ms

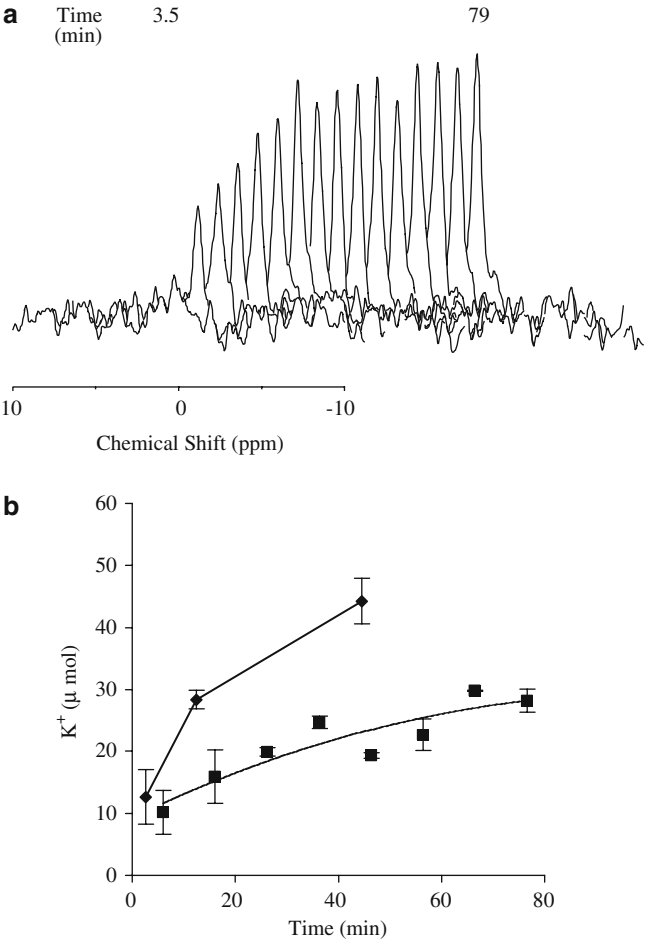

Fig. 4 Extracellular $^{39}K^+$ in suspensions of RBCs following activation of the Gárdos channel. **a** Washed RBCs were suspended in K^+-free medium. At time = 0, 30 μL of 0.8 mM A23187 in DMSO and 30 μL of 51.63 mM $CaCl_2$ were added to 3 mL of the cells (Ht = 0.61). Spectra were acquired using the inversion-recovery pulse sequence where τ_1 was chosen such that the intracellular magnetization vector in the z-direction was 0 as the final 90° pulse was applied. **b** Relative signal intensity calculated from the integrals of the ^{39}K inversion-recovery spectra. The *solid line* represents a quadratic function that was regressed onto the NMR data (*filled squares*). The calculated initial rate was 0.213 ± 0.084 mmol (L RBCs)$^{-1}$ min^{-1}. A similar experiment performed using AAS (initial Ht = 0.55) yielded an initial rate estimate of 1.19 ± 0.40 mmol (L RBCs)$^{-1}$ min^{-1} (*filled diamonds*). Data points are the average of two consecutive spectra. *Error bars* represent ±1SD

Dependence of T_1 on RBC volume

If RBCs are suspended in a hypotonic solution, water will rapidly redistribute across the membrane (via aquaporin) such that the osmotic pressure is the same on

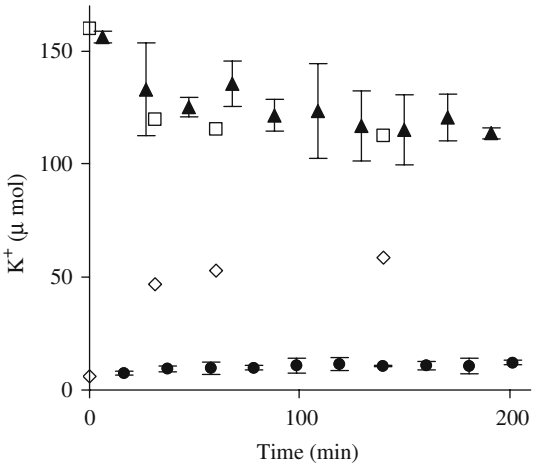

Fig. 5 Gárdos channel-mediated K^+ flux in RBCs measured using AAS or NMR inversion-recovery pulse sequences. Three millilitres of washed RBCs were suspended in HBS supplemented with 10 mM glucose (Ht = 0.68). At time = 0, 30 μL of 0.8 mM A23187 in DMSO and 30 μL of 51.63 mM $CaCl_2$ were added to the tube. Three hundred microlitre aliquots were taken at the times indicated. The initial $[K^+]_{in}$ in this experiment was determined to be 110 mmol (L cell water)$^{-1}$. Regression of monoexponential functions onto the NMR data yielded an initial K^+ efflux rate of 0.110 ± 0.85 mmol (L RBC)$^{-1}$ min^{-1}. When the same experiment was performed and $[K^+]$ measured by AAS the initial rate of efflux was 1.154 ± 0.005 mmol (L RBC)$^{-1}$ min^{-1}. Intra- and extracellular K^+ amounts as measured by AAS are denoted by *open squares*, and *open diamonds*, respectively. NMR data were acquired using the inversion-recovery pulse sequence with τ_1 set to either 11 ms (*filled circles*) or 40 ms (*filled triangles*). *Data points* represent the average of two experiments. *Error bars* are $\pm$1SD

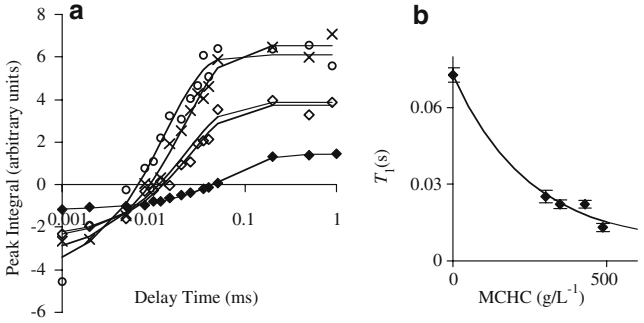

Fig. 6 $T_{1,in}$ of $^{39}K^+$ in RBCs of various volumes. RBCs were prepared as described in the Methods. Two millilitre aliquots of Ht = 0.9 were added to 1 mL of hypo-, hyper- or isotonic saline. The final Ht was measured by capillary centrifugation and this was used to calculate the intracellular [Hb]. The MCHCs were (in g L^{-1}): *filled diamonds* 300, *open triangles* 347.1, *crosses* 428.6, *open diamonds* 488.4 and *open circles* 0. **a** *Unbroken lines* denote least-squares regression of the function $S(t) = S(\infty) - (S(\infty) - S(0))\, e^{-t_1/T_1}$ onto the data *filled diamonds* $S(\infty) = 3.75$, $a = 1.66$, $T_1 = 0.025$; *open triangles* $S(\infty) = 3.87$, $a = 1.67$, $T_1 = 0.0223$; *crosses* $S(\infty) = 6.53$, $a = 1.51$, $T_1 = 0.0222$; *open squares* $S(\infty) = 6.11$, $a = 1.68$, $T_1 = 0.0131$; *open circles* $S(\infty) = 1.434$, $a = 1.82$, $T_1 = 0.0728$. **b** T_1 values extracted from the data in (**a**) against the MCHC. The *solid line* is the least squares regression of the function $T_{1,in} = T_{1,0}\, e^{-k[Hb]} + C$ onto the data where $T_{1,0} = 0.06619$, $k = 0.00405$ and $C = 0.00656$. *Error bars* are residuals from the 3-parameter fit calculated in *Mathematica*

both sides of the membrane. This results in an increase in the water content inside the cells, and hence a decrease in [Hb]. The opposite case applies to cells suspended in a hypertonic solution. If the Ht is measured by capillary centrifugation before and after the addition of diluted or concentrated HBS to the suspension, the [Hb] inside the cells can be estimated using the equation:

$$[Hb]_{in} = MCHC_0 \times \frac{Vol_T Ht_0 - Vol_\alpha}{Vol_T Ht_1 - Vol_\alpha}, \quad (6)$$

where $MCHC_0$ is the mean corpuscular haemoglobin concentration at time = 0, Vol_T is the total volume of the suspension, Vol_α is the volume of the cells occupied by Hb, Ht_0 is the initial Ht, and Ht_1 is the Ht measured after addition of modified HBS.

The dependence of the T_1 of $^{39}K^+$ inside the cells, T_{1in}, on haemoglobin concentration, [Hb], was investigated by measuring the T_1 value in RBCs swollen or shrunken in hypo- or hypertonic solutions, respectively (Fig. 6a). Figure 6b shows the regression of the following expression onto the data:

$$T_{1,in} = T_{1,0}\, e^{-k[Hb]} + C, \quad (7)$$

where $T_{1,0}$ is the T_1 of $^{39}K^+$ when [Hb] = 0, and k and C are phenomenological constants. The measured value of $T_{1,0}$ was 72.8 ms. Equation 7 was then used to generate an expression to describe the intensity of the ^{39}K NMR resonance from an inversion-recovery pulse sequence at any given cell volume.

The intensity of the total inversion recovery $^{39}K^+$ signal, S_{IR} (which is time-dependent) from a suspension of RBCs can be considered a superposition of the time-dependent signals from outside, $s_{out}(t)$, and inside, $s_{in}(t)$, the cells:

$$S_{IR}(t) = s_{out}(t) + s_{in}(t). \quad (8)$$

The value of $s_{in}(t)$ is given by:

$$s_{in}(t) = Q\, K^+_{in}(t)\, (1 - a\, e^{-\tau_1/T_{1,in}})/(K^+_{in}(t) + K^+_{out}(t)), \quad (9)$$

where a is a constant and Q is a scalar that relates the signal intensity to K^+ concentration; noting that in natural systems ^{39}K is 93.9% and ^{41}K is 6.1% of all the potassium present, and similarly:

$$s_{in}(t) = Q\, K^+_{out}(t)\, (1 - a\, e^{-\tau_1/T_{1,out}})/(K^+_{in}(t) + K^+_{out}(t)). \quad (10)$$

Figure 7 shows the same experimental data as displayed in Figure 5 (error bars have been removed for clarity), along with amounts of intra- and extracellular K^+ predicted by the simulation. It was found that the AAS data (open symbols) closely matched the output from the model for the amounts of K^+ (broken traces). When the same simulated data were entered into Eq. 9 (setting τ_1 to 11 ms, lower solid trace) and Eq. 10

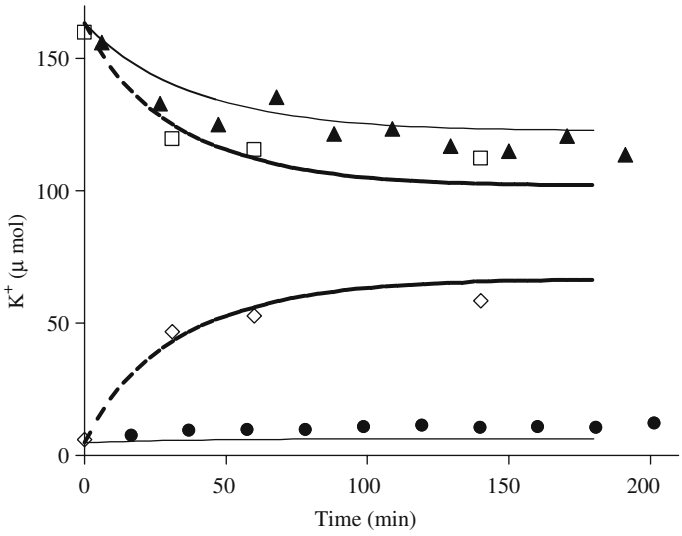

Fig. 7 Comparison between simulation and experiment for Gárdos channel flux data from NMR and AAS. The *solid* and *broken lines* represent simulation of the NMR and AAS data, respectively, from Fig. 5; *error bars* from the latter were omitted for clarity

(setting τ_1 to 40 ms, upper solid trace), there was a close resemblance to the NMR data (filled symbols).

Discussion

Nuclear magnetic resonance continues to be an information-rich method for studying monovalent cations in RBC suspensions (Resnick et al. 2001). Our approach in this report has been to develop further the NMR techniques that are used to measure, in particular, K^+ in separate compartments in RBC suspensions. Despite its relatively low magnetogyric ratio, the ^{39}K nucleus can yield unique information on the distribution of the ion in suspensions of RBCs. Our estimates of transport rates were consistent with previous studies on other cell types, and showed that differences in the longitudinal relaxation times in RBC suspensions can be used to observe selectively $^{39}K^+$ in either compartment. This approach was complicated by the need to consider the time-dependent changes in cell volume. To our knowledge, this is the first example of using the inversion-recovery pulse sequences to observe $^{39}K^+$ transport in RBCs, and in particular, the observation of changes in extracellular $^{39}K^+$.

Our aim was to approach the problem of measuring the net ion transport across the RBC membranes by using two distinct but relatable methods. AAS is a highly sensitive and well established method and is used to measure $[K^+]$ very reliably. Time-dependent analysis of the changes in $[K^+]$ in compartments in an RBC suspension, however, can be a very invasive process, and may not be reflective of the active (unbound) $[K^+]$.

The central method was NMR. Although the Boltzmann distribution of its ^{39}K spins renders this technique inherently insensitive, it has the merit of being non-invasive. In this work, we exploited the shorter relaxation time, T_1, of $^{39}K^+_{in}$, caused by increased viscosity of the cytoplasm and interaction of the $^{39}K^+$ ions with proteins (Seo et al. 1987). Hence, we refined the method and demonstrated a selective detection and time-dependent measurement of net $^{39}K^+$ transport in RBC suspensions.

For data analysis, mathematical modelling served as a convenient means of interrelating the results of the two distinct experimental approaches. Figure 7 shows that the model was able to describe both the AAS and NMR data from the experiments performed under similar conditions. Thus, it was used in conjunction with the NMR experiments to give reliable information on the time-dependence of $[K^+]$ in RBC suspensions.

It is not possible to obtain an analytical solution to the system of DEs defined in the model (only a numerical solution is obtainable), thus prohibiting a direct nonlinear regression of an expression onto the data. Development of parameter-refinement techniques [such as those described in Mulquiney and Kuchel (2003)] should facilitate the calculation of rate constants from data obtained by various experimental techniques. A future development of this work will be the incorporation of the data into our detailed kinetic model of RBC metabolism (Mulquiney et al. 1999; Mulquiney and Kuchel 1999a, b, 2003).

A broader implication of this work is an understanding of the physiological role of the Gárdos channel. The $[Ca^{2+}]_{free}$ inside the cells is normally maintained at ~60 nM in circulating RBCs (Murphy et al. 1986), well below the threshold for activation of the channel. It is known that the Gárdos channel is a major contributor to the dehydration reactions of RBCs of the patients with SSA but much remains to be deciphered regarding its physiological role. The results presented here show that K^+ loss (and hence water loss) from the cells via this pathway occurs over a time-scale of hours following Ca^{2+} activation. Thus, assuming the Gárdos channel has a role in the deformation of cells in the microcapillary circulation, it would most likely operate in concert with the other K^+ pathways, the K^+/Cl^- and $Na^+/K^+/2Cl^-$ co-transporters. It also cannot be ruled out that the activation of the Gárdos channel is involved in the

'tagging' of RBCs as 'aged', and hence their subsequent removal from the circulation.

In conclusion, we have presented a non-invasive NMR method that was used to measure net K^+ transport in RBC suspensions; and we developed a mathematical model that can be used to aid the interpretation of ^{39}K NMR experiments. This led to an estimate of the real efflux rate of K^+ under several experimental conditions; these flux estimates will be useful in formulating quantitative models of RBC metabolism.

Acknowledgements This work was supported by a grant from the Australian National Health and Medical Research Council and the Australian Research Council to PWK. ADM was the recipient of a University of Sydney Postgraduate Award. Mr Bill Lowe is thanked for expert technical assistance and Dr Bill Bubb for assistance with the NMR spectrometers.

Appendix

The model describes the time-dependence of the distribution of certain ions and water in a suspension of RBCs following activation of the Gárdos channel by Ca^{2+}_{in}. This is essentially a two-compartment system in which the rates of chemical and physical (membrane transport) reactions can be modelled as ordinary differential equations (ODEs).

Input

The first step was to define the experimental parameters of total volume of suspension, and Ht. From this the ion and water distribution can be calculated assuming 30% of the initial intracellular volume is occupied by Hb. The initial concentrations of K^+_{in}, K^+_{out}, Ca^{2+}_{in}, and Ca^{2+}_{out} were defined as 115 mM, 60 nM, 5 mM and 2 mM, respectively. Na^+ concentrations in both compartments were defined as 154 mM minus the initial K^+ concentration in the respective compartment. Initial [Hb] was defined as 5 mM, and the contribution of impermeant intracellular solutes was defined as 30 mM. It was assumed that the charge on each Hb molecule was -2. Initial $[A23187]_{out}$ was defined as 22 μM. Initial concentration of non-specific intracellular Ca^{2+} buffers were set to 1 mM, with a dissociation constant of 10 μM. The time dependence of the intracellular volume was defined according to Eq. 5 (see Methods).

Unitary rate constants were defined for K^+ and Na^+ transport through the Gárdos channel as 0.286×10^{-3} s^{-1}, and 0 s^{-1}, respectively. Unitary rate constants were also multiplied by the square root of the $[Cl^-]_{in}$:$[Cl^-]_{out}$ ratio (Rohwer et al. 2002). The amount of Cl^- in both compartments was defined as the sum of the amount of K^+ and Na^+ (minus the number of negative charges on Hb inside the cell). The rate of transport of Ca^{2+} into the cells was defined in terms of the [A23187].

The general format for membrane transport rate equations was:

$$v_C = \frac{k_{Cio}C}{1 + \left(\frac{K_{ac}}{[Ca^{2+}_{in}]}\right)} - \frac{k_{Coi}C}{1 + \left(\frac{K_{ac}}{[Ca^{2+}_{in}]}\right)}, \quad (11)$$

where C denotes a particular cation (K^+ or Na^+), K_{ac} is the activation constant for Ca^{2+}_{in}, and k_{Cio} is the unitary rate constant for cation C in the 'in to out' direction; the rate constant with subscript 'oi' refers to the 'out to in' direction.

The time-course was modelled as 10 ODEs using the built-in function NDSolve over a simulated time course of 4 h. This function iteratively finds a numerical solution to the defined ODEs by a predictor-corrector method.

Analysis

The NDSolve function stores the solution of the system of ODEs as an 'InterpolatingFunction'. The time-dependence of any of the metabolites can be checked using the Plot function. Once it was established that the model described the defined system sufficiently well, equations were entered to describe the T_1 in terms of the intracellular [Hb], with a view to modelling the time-dependence of the ^{39}K NMR signal acquired with an inversion-recovery pulse sequence at any given delay time τ_1.

The first step was to define Eq. 7 (see Results), with [Hb] given by:

$$[Hb] = MCHC_0 \times \frac{Vol_{in,0}}{Vol_{in}}, \quad (12)$$

where $MCHC_0$ is the MCHC at time = 0, $Vol_{in,0}$ is the intracellular volume at time = 0 and Vol_{in} is the intracellular volume at time t. Equation 7 was then defined with $T_{1,0}$, k and C taking the experimentally determined values of 0.6619 s, 0.00405 and 0.00656, respectively. Equations describing the time-dependence of the ^{39}K NMR signal were then defined (see Eqs. 8, 9 and 10). The simulated output was directly compared to the experimental data using the Plot function.

The *Mathematica* Notebook that contains the above model is available as an email attachment from the authors.

References

Brugnara C (1995) Erythrocyte dehydration in pathophysiology and treatment of sickle cell disease. Curr Op Hematol 2:132–138

Brugnara C, Bunn HF, Tosteson DC (1986) Regulation of erythrocyte cation and water content in sickle cell anemia. Science 232:388–390

Bydder GM (1992) Technical advances in magnetic resonance imaging. Curr Op Neurol Neurosug 5:854–858

Bydder GM, Hajnal JV, Young IR (1998) MRI: use of the inversion recovery pulse sequence. Clin Radiol 53:159–176

Gupta RK, Gupta P (1982) Direct observation of resolved resonances from intra- and extracellular sodium-23 ions in NMR studies of intact cells and tissues using dysprosium (III) tripolyphosphate as paramagnetic shift reagent. J Magn Reson 47:344–350

Hiraishi T, Seo Y, Murakami M, Watari H (1990) Detection of biexponential relaxation in intracellular K in the rat heart by double-quantum ^{39}K NMR. J. Magn Reson 87:169–173

Joyner SE, Kirk K (1994) Two pathways for choline transport in eel erythrocytes: a saturable carrier and a volume-activated channel. Am J Physiol 267:R773–R779

Kates R, Atkinson D, Brant-Zawadzki M (1996) Fluid-attenuated inversion recovery (FLAIR): clinical prospectus of current and future applications. Top Magn Reson Imaging 8:389–396

Knubovets TL, Revazov AV, Sibeldina LA, Eichhoff U (1989) ^{23}Na NMR measurement of the maximal rate of active sodium efflux from human red blood cells. Magn Reson Med 9:261–272

Kuki S, Suzuki E, Watari H, Takami H, Matsuda H, Kawashima Y (1990) Potassium-39 nuclear magnetic resonance observation of intracellular potassium without chemical shift reagents during metabolic inhibition in the isolated perfused rat heart. Circ Res 67:401–405

Mulquiney PJ, Bubb WA, Kuchel PW (1999) Model of 2,3-bisphosphoglycerate metabolism in the human erythrocyte based on detailed enzyme kinetic equations: in vivo kinetic characterization of 2,3-bisphosphoglycerate synthase/phosphatase using ^{13}C and ^{31}P NMR. Biochem J 342:567–580

Mulquiney PJ, Kuchel PW (1999a) Model of 2,3-bisphosphoglycerate metabolism in the human erythrocyte based on detailed enzyme kinetic equations: equations and parameter refinement. Biochem J 342:581–596

Mulquiney PJ, Kuchel PW (1999b) Model of 2,3-bisphosphoglycerate metabolism in the human erythrocyte based on detailed enzyme kinetic equations: computer simulation and metabolic control analysis. Biochem J 342:597–604

Mulquiney PJ, Kuchel PW (2003) Modelling metabolism with *Mathematica*. CRC Press, Boca Raton, FL

Murphy E, Levy L, Berkowitz LR, Orringer EP, Gabel SA, London RE (1986) Nuclear magnetic resonance measurement of cytosolic free calcium levels in human red blood cells. Am J Physiol 251:C496–C504

Murakami M, Suzuki E, Miyamoto S, Seo Y, Watari H (1989) Direct measurement of K movement by ^{39}K NMR in perfused rat mandibular salivary gland stimulated with acetylcholine. Pflugers Archiv 414:385–392

Newhouse JH (1986) Image contrast and pulse sequences in urinary tract magnetic resonance imaging. Urologic Radiol 8:120–126

Pettegrew JW, Woessner DE, Minshew NJ, Glonek T (1984) Sodium-23 NMR analysis of human whole blood, erythrocytes and plasma. Chemical shift, spin relaxation and intracellular sodium concentration studies. J Magn Reson 57:185–196

Pike MM, Frazer JC, Dedrick DF, Ingwall JS, Allen PD, Springer CS Jr, Smith TW (1985) ^{23}Na and ^{39}K nuclear magnetic resonance studies of perfused rat hearts. Discrimination of intra- and extracellular ions using a shift reagent. Biophys J 48:159–173

Pike MM, Simon SR, Balschi JA, Springer CS Jr (1982) High-resolution NMR studies of transmembrane cation transport: use of an aqueous shift reagent for ^{23}Na. Proc Natl Acad Sci USA 79:810–814

Preston E, Foster DO (1993) Diffusion into rat brain of contrast and shift reagents for magnetic resonance imaging and spectroscopy. NMR Biomed 6:339–344

Resnick LM, Barbagallo M, Dominguez LJ, Veniero JM, Nicholson JP, Gupta RK (2001) Relation of cellular potassium to other mineral ions in hypertension and diabetes. Hyperten 38:709–712

Rohwer JM, Kuchel PW, Maher AD (2002) Thermokinetic modelling: membrane potential as a dependent variable in ion transport processes. Mol Biol Rep 29:217–225

Seo Y, Murakami M, Suzuki E, Watari H (1987) A new method to discriminate intracellular and extracellular K by ^{39}K NMR without chemical-shift reagents. J Magn Reson 75:529–533

Seo Y, Murakami M, Suzuki E, Kuki S, Nagayama K, Watari H (1990) NMR characteristics of intracellular K in the rat salivary gland: a ^{39}K NMR study using double-quantum filtering. Biochemistry 29:599–603

Shedd SF, Spicer LD (1991) Characterization of a microcarrier cell culture system for ^{23}Na MR spectroscopy studies. NMR Biomed 4:246–253

Weidensteiner C, Horn M, Fekete E, Neubauer S, von Kienlin M (2002) Imaging of intracellular sodium with shift reagent aided (23)Na CSI in isolated rat hearts. Magn Reson Med 48:89–96

Yingst DR, Hoffman JF (1984) Ca-induced K transport in human red blood cell ghosts containing arsenazo III. Transmembrane interactions of Na, K, and Ca and the relationship to the functioning Na-K pump. J Gen Physiol 83:19–45